ROYAL SOCIETY OF CHEMISTRY

PCCP

The Pure Rotational Spectrum of the T-Shaped AlC$_2$ Radical (X̃ ^{2}A$_1$)

SCHOLARONE™
Manuscripts

The Pure Rotational Spectrum of the T-Shaped AlC$_2$ Radical

($\tilde{X}^2$A$_1$)

D. T. Halfen and L. M. Ziurys

Department of Chemistry and Biochemistry,

Department of Astronomy,

and Steward Observatory,

University of Arizona,

1305 E. 4th Street

Tucson, AZ 85719

Phone: 520-626-0701

Fax: 520-621-5554

email: halfend@email.arizona.edu

Abstract

The pure rotational spectrum of the AlC_2 radical ($\tilde{X}^2A_1$) has been measured using Fourier transform microwave/millimeter-wave (FTMmmW) techniques in the frequency range $21 - 65$ GHz. This study is the first high-resolution spectroscopic investigation of this molecule. AlC_2 was created in a supersonic jet from the reaction of aluminum, generated by laser ablation, with a mixture of CH_4 or HCCH, diluted in argon, in the presence of a DC discharge. Three transitions ($N_{K_aK_c} = 1_{01} \rightarrow 0_{00}$, $2_{02} \rightarrow 1_{01}$, and $3_{03} \rightarrow 2_{02}$) were measured, each consisting of multiple fine/hyperfine components, resulting from the unpaired electron in the species and the aluminum-27 nuclear spin ($I = 5/2$). The data were analyzed using an asymmetric top Hamiltonian and rotational, fine structure, and hyperfine constants determined. These parameters agree well with those derived from previous theoretical calculations and optical spectra. An r_0 structure of AlC_2 was determined with $r(Al–C) = 1.924$ Å, $r(C–C) = 1.260$ Å, and $\theta(C–Al–C) = 38.2^o$. The Al-C bond was found to be significantly shorter than in other small, Al-bearing species. The Fermi contact term established in this work indicates that the unpaired electron in the valence orbital has considerable $3p_za_1$ character, suggesting polarization towards the C_2 moiety. A high degree of ionic character in the molecule is also evident from the quadrupole coupling constant. These results are consistent with a T-shaped geometry and an $Al^+C_2^-$ bonding scheme. AlC_2 is a possible interstellar molecule that may be present in the circumstellar envelopes of carbon-rich AGB stars.

Introduction

Dicarbide species containing a single heteroatom are common in interstellar and circumstellar gas, including such species as CCN, CCO, CCP, CCS, and SiC_2.[1-5] Because of their astrophysical relevance, as well as their varied structures, these molecules have been the subject of many experimental and theoretical investigations in recent years. Spectroscopic measurements have shown that some of these species have simple linear geometries, such as CCN, CCO, and CCP.[6-8] Experimental and theoretical studies have indicated that others are slightly bent, including CCCl and CCF, which exhibit bond angles of $\theta = 157$ and 165°, respectively.[9,10] In addition, a number of cyclic-like structures are present in the dicarbide molecules. Rotational spectroscopy has revealed T-shaped geometries with $M-C_2$ bonding for SiC_2, ScC_2, YC_2 and GeC_2, for example,[11-14] while theory predicts TiC_2, CoC_2, and NiC_2 to be true ring structures with two metal-carbon bonds.[15] Calculations have also shown some propensity for L-shaped configurations in the dicarbides. For example, Sari et al. predicted the M-C-C bond angle for GeC_2 to be in the range of $\theta = 80 - 100^o$, depending on the level of theory.[16] The metal-containing dicarbides are of particular note, as these species are also thought to be involved in the formation of metallo-carbohedrenes (met-cars).[17,18]

Another metal dicarbide of interest is the AlC_2 radical. This species was initially detected in the laboratory by mass spectrometry, argon matrix-ESR techniques and photoelectron spectroscopy;[19,20] more recently, electronic spectra of this molecule have been measured using laser-induced fluorescence (LIF).[21-23] In addition, several theoretical studies have computed the ground electronic state ($\tilde{X}^2A_1$) geometry, the barrier to linearity, and other spectroscopic paremeters.[23,24] The most current experimental work on AlC_2 is by Yang et al., who measured 18 vibronic bands of the $C^2B_2 - \tilde{X}^2A_1$ transition with LIF, recording high-resolution spectra of

3

the 0^0_0 system.[23] From these data, rotational and Al hyperfine constants for the ground and excited states of AlC_2 were derived – the most accurate parameters for this molecule to date. In addition, Yang et al. performed high-level theoretical calculations for the radical, deriving a structure, dipole moment, vibrational frequencies, and rotational, fine structure, and hyperfine constants.[23]

Here we present the first measurements of the pure rotational spectrum of the AlC_2 radical in its $\tilde{X}^2A_1$ ground electronic state. These data were recorded using Fourier transform microwave/millimeter-wave (FTMmmW) techniques over the frequency range 21 – 65 GHz. Innovative instrumentation spanning the U- and E-bands (40 – 60 GHz and 60 – 90 GHz) were employed for the millimeter-wave measurements.[12] In the three rotational transitions studied, hyperfine interactions, arising from the aluminum nuclear spin of $I = 5/2$, were readily resolved, allowing for a very accurate determination of the spectroscopic parameters of this radical. The data are consistent with a T-shaped structure for AlC_2, with the unpaired electron principally located on the aluminum nucleus. Here we present our measurements, spectroscopic analysis and interpretation, as well as accurate rest frequencies of this radical for future astronomical studies.

Experimental

The rotational spectrum of AlC_2 was recorded using the Fourier transform microwave/ millimeter wave (FTMmmW) spectrometer of the Ziurys group. This Balle-Flygare-type instrument consists of a vacuum chamber that contains a Fabry-Pérot cavity with two spherical aluminum mirrors in a near-confocal arrangement. Two sets of mirrors are used to cover the full frequency range (4 – 90 GHz) of the instrument.[12,25] For 4 – 40 GHz operation, antennas are imbedded in two 20 inch diameter mirrors for injection of microwave signals and detection of

molecular emission; above 40 GHz, waveguide, mounted in two 6.7 inch diameter mirrors, are used to couple radiation into the cell and then collect subsequent emission. A synthesizer (Agilent) directly generates signals for the 4 – 40 GHz range; higher frequencies are attained by multiplying the synthesizer output using either doublers (40 – 60 GHz & 60 – 75 GHz: Norden Millimeter) or a quadrupler (75 – 90 GHz: Norden Millimeter). Gas-phase molecules are directed into the cavity using a pulsed, supersonic nozzle (General Valve), oriented 40° relative to the optical axis and operating at 10 Hz. Molecular emission is detected in the time domain (the Free Induction Decay or FID) using one of four low noise amplifiers (Miteq, Spacek, Norden Millimeter, NRAO), depending on the frequency band. Spectra are then generated by a Fast Fourier transform (FFT) of the FID with a 4 kHz frequency resolution. Details can be found in Ref. 25.

AlC_2 was produced using a discharge-assisted laser ablation source (DALAS). DALAS consists of a supersonic pulse value attached to an ablation apparatus (rotating/translating metal rod, ablated by a Nd:YAG laser) with a DC discharge nozzle at the output.[26,27] The second-harmonic of a Nd/YAG laser (Continuum Surelite II) is used at 532 nm with a typical power of 200 mJ/pulse. To create AlC_2, a mixture of 0.5% methane or 0.125% acetylene in argon was expanded from the nozzle at a stagnation pressure of ~40 psi and flow of 20 – 40 sccm. The mixture was flowed into the ablation region, entraining gaseous metal vaporized from an aluminum rod (Aldrich), and then through the DC discharge nozzle into the cavity. The discharge voltage was set to 850 V. To achieve an adequate signal-to-noise ratio, 500 to 10,000 pulse averages were accumulated and averaged. Each line is recorded as a Doppler doublet as a result of the alignment of the molecular expansion relative to the cavity axis. The center of this doublet is the transition frequency.

Results

AlC$_2$ is an asymmetric top molecule in the C_{2v} point group with a ^{2}A$_1$ ground electronic state and a T-shaped geometry, according to previous work.[23] Each rotational level is therefore labeled by $N_{K_aK_c}$, where N is the rotational angular momentum and K_a and K_c are its projections along the $\hat{a}$ and $\hat{c}$ molecular axes. This species also has one unpaired electron, located in an a_1 orbital, and therefore $S = 1/2$. In a case b_{β_J} coupling scheme, S couples to N to produce fine structure doublets for each $N_{K_aK_c}$ level, indicated by quantum number J, where $\boldsymbol{J} = \boldsymbol{N} + \boldsymbol{S}$. The nuclear spin I then adds to J to generate hyperfine levels, labeled by total angular momentum quantum number F, where $\boldsymbol{F} = \boldsymbol{J} + \boldsymbol{I}$; see Figure 1. However, because the aluminum-27 nucleus has a spin of $I = 5/2$ and a large magnetic moment of 3.64 μ_N,[28] an alternative coupling scheme for AlC$_2$ is case b_{β_S}. Here S and I couple first to create angular momentum G, which in turn adds to N to create F, i.e. $\boldsymbol{G} = \boldsymbol{S} + \boldsymbol{I}$ and $\boldsymbol{F} = \boldsymbol{N} + \boldsymbol{G}$. In either case the most favorable rotational transitions correspond to $\Delta F = 0, \pm 1$. Further complications arise because the two ^{12}C nuclei are identical bosons each with $I = 0$. Therefore, the total molecular wave function for this molecule must be symmetric with respect to particle exchange, which, for A$_1$ ground electronic and vibrational states, means that rotational levels with only even K_a quantum numbers exist (i.e. K_a = 0, 2, 4, etc); levels with odd K_a values are not present. Figure 1 shows the resulting energy level diagram for AlC$_2$ and the molecule's complex hyperfine structure. The figure also displays the correlation diagram between the two coupling schemes for the N = 0, 1, and 2 rotational levels. The focus of this study is transitions between these levels, as well those involving N = 3.

The search for the rotational spectrum of AlC$_2$ was based on predicted frequencies using the spectroscopic constants calculated at the B3LYP/aug-cc-pV(5 + d)Z level by the Clouthier group.[23,29] Initially, hyperfine lines originating in the $N = 1 \rightarrow 0$, $K_a = 0$ transition of AlC$_2$ were

searched for near 21.8 GHz. Three spectral features near 21817 MHz, 21819 MHz, and 21733

MHz were first found, but searches for additional lines were unsuccessful. Fortunately, at this

time the FTMW spectrometer was upgraded to operate in the $40 - 60$ GHz and $60 - 90$ GHz

regions (U and E bands). Subsequent measurements revealed spectral features near 43.5 GHz

and 65.1 GHz, originating in the $N = 2 \rightarrow 1$ and $N = 3 \rightarrow 2$ transitions. With this higher

frequency data in hand, a spectral analysis could be performed with sufficient accuracy that a

more targeted search could be performed for additional hyperfine lines of the $N = 1 \rightarrow 0$ and 2

$\rightarrow 1$ transitions. Chemical tests were performed for all measured features to insure that they

were due to the metal and CH_4, and required the DC discharge – all indications of a radical

species containing Al and C. The chemical behavior of the lines also mimicked those measured

for YC_2 and ScC_2 from our previous studies, another important check.

A list of the transitions measured for AlC_2 is given in Table 1. A total of 23

fine/hyperfine components were recorded across three rotational transitions in the frequency

range $21 - 65$ GHz. The measured lines all arise from the $K_a = 0$ asymmetry component and

follow the selection rules $\Delta J = 0, \pm 1, \pm 2$ and $\Delta F = 0, \pm 1$. Figure 1 displays the measured

transitions in the $N = 0, 1,$ and 2 manifold.

Representative spectra of AlC_2 are displayed in Figure 2. Brackets present above each

spectral feature designate the Doppler doublets. The top panel shows the $N_{K_a,K_c} = 1_{01} \rightarrow 0_{00}$

transition near $21.7 - 21.9$ GHz. Four of the six measured fine/hyperfine components of this

transition are shown, labeled by quantum numbers J and F; two features arise from the $J = 0.5 \rightarrow$

0.5 spin-rotation set and the remaining two correspond to $J = 1.5 \rightarrow 0.5$. The middle panel

displays four of the 13 lines recorded for the $N_{K_a,K_c} = 2_{02} \rightarrow 1_{01}$ transition near $43.5 - 43.6$ GHz.

Here two components come from the $J = 2.5 \rightarrow 1.5$ spin-rotation group, and the others

correspond to $J = 1.5 \rightarrow 1.5$ and $J = 1.5 \rightarrow 0.5$, as labeled in the figure. The bottom panel

presents spectra obtained for the $N_{K_a,K_c} = 3_{03} \rightarrow 2_{02}$ transition near $65.1 - 65.2$ GHz. All four

hyperfine components recorded in transition are displayed, three from the $J = 3.5 \rightarrow 2.5$ spin-

rotation group, and the other from $J = 2.5 \rightarrow 2.5$ (see Table 1). Note that there are three

frequency breaks in all data sets presented. Also, the lines are plotted on the same intensity scale

within each panel.

The measured transition frequencies for AlC_2 were analyzed using an A-reduced

asymmetric top Watson Hamiltonian.[30] The A-reduction Hamiltonian was chosen to allow for a

direct comparison to the theoretically-calculated values, and has been shown to produce precise

constants for other dicarbide species, such as YC_2 and ScC_2.[12,13] The Hamiltonian comprises

rotation, centrifugal distortion, spin-rotation, magnetic hyperfine, and electric quadrupole

interactions:

$$\hat{H}_{eff} = \hat{H}_{rot} + \hat{H}_{cd} + \hat{H}_{sr} + \hat{H}_{mhf} + \hat{H}_{eQq} . \tag{1}$$

The data were fit using a non-linear least-squares method as implemented in SPFIT.[31] The

resulting spectroscopic constants are given in Table 2, along with their corresponding 3σ errors

as determined in the analysis.

Due to the C_{2v} symmetry, only diagonal elements of the spin-rotation (ε_{aa}, ε_{bb}, and ε_{cc})

and nuclear spin-rotation tensors (C_{aa}, C_{bb} and C_{cc}) exist for AlC_2, which simplifies the

analysis.[32] However, as only the $K_a = 0$ asymmetry component transitions were recorded for

each rotational state, a number of constants had to be kept at the theoretical values, namely, the

rotational constant A, the centrifugal distortion parameters Δ_{NK}, Δ_K, δ_N, and δ_K, the spin-rotation

term ε_{aa}, and the nuclear spin-rotation constant C_{aa}. Measurement of other asymmetry

components would be necessary to determine these constants accurately and/or independently.

As another consequence, the parameter Δ_N is an effective value, applicable only to the $K_a = 0$ component of AlC_2. Also, the ratios of B and C, ε_{bb} and ε_{cc}, and C_{bb} and C_{cc} were kept at the values set by the theoretical constants.[23,29] The Fermi contact term a_F and components of the dipolar and quadrupole tensors were determined in the fit, as well. Again, because of the C_{2v} symmetry, only two of the three diagonal terms in these two tensors can be established independently.[33] The dipolar constants T_{aa} and $T_{bb} - T_{cc}$ were indeed successfully determined from the data set. Note that $T_{aa} + T_{bb} + T_{cc} = 0$. For the quadrupole tensor, on the other hand, only χ_{aa} could be discerned from the analysis. Attempts to determine the term χ_{bb} - χ_{cc} produced undefined values. A centrifugal distortion correction to the Fermi contact constant a_{FD} was found necessary for the analysis, as well. The final *rms* value of the fit is 3 kHz, within the estimated experimental uncertainty of ±4 kHz.

The experimentally-determined spectroscopic constants for AlC_2 established here are in good agreement with those from previous theoretical calculations.[23,29] The rotational constants B and C are within 1.7% of the theoretical values, as are the hyperfine constants T_{aa}, C_{bb}, and C_{cc}. The Fermi contact term a_F varies by about 9%, and the spin-rotation constants ε_{bb} and ε_{cc} have a 14% difference, from the calculated parameters. In addition, the experimentally-determined Fermi contact term from Yang et al.[23] of $a_F = 947(54)$ MHz is consistent with our value of $a_F = 958.2(2.3)$ MHz within experimental error. The measured rotational constants B and C from Yang et al. are within 1.4% of our values, but this comparison is only qualitative as the ratio of these constants was fixed in our analysis.[23]

Discussion

The spectra measured here for AlC_2 are consistent with the T-shape geometry proposed by previous experimental and theoretical works. The good agreement between the spectroscopic

constants from Yang et al. and those determined here support this conclusion.[23] Furthermore, the

higher-energy linear structure of AlCC calculated by Largo et al. had an estimated rotational

constant of ~5700 MHz,[34] quite different from the effective B of ~10.9 GHz established in this

study.

From this work, a structure of AlC_2 can be calculated. Using the theoretical value for A

and the experimental values of B and C listed in Table 2, an r_0 geometry for AlC_2 was evaluated

using the STRFIT code.[35] The results suggest $r(Al–C) = 1.924$ Å, $r(C–C) = 1.260$ Å, and $\theta(C–$

$Al–C) = 38.2^{\circ}$. In contrast, the Al-C bond distances in AlCCH and $AlCH_3$ are 1.963 Å and 1.980

Å, respectively,[36,37] – significantly longer. For both these molecules, the aluminum atom appears

to make a single bond to the acetylide or methyl moiety. The shorter Al-C distance in AlC_2

suggests an alternative bonding scheme.

The C-C bond length in AlC_2 is very similar to that of SiC_2, ScC_2, and YC_2 at ~1.26 –

1.27 Å.[11-13] This value is intermediate between that found in HCCH (1.20241(9) Å) and

CH_2CH_2 (1.3391(13) Å),[38,39] and longer than that of neutral C_2 (1.2425 Å).[39] However, it is very

similar to the bond length of C_2^{-} (1.2682 Å).[40] Therefore, the structure that perhaps best

represents the molecule is $Al^{+}C_2^{-}$, with the unpaired electron being principally located near the

C_2 moiety, as suggested by theory.[24,34] This ionic scheme is consistent with the T-shape

geometry and the short Al-C bond length.

The electron configuration for AlC_2 is calculated to be (core) $5a_1{}^{2}6a_1{}^{2}3b_2{}^{2}2b_1{}^{2}7a_1{}^{2}8a_1{}^{1}$.[34]

Given the geometry, the valence $8a_1$ orbital is likely a mixture of Al $3p_z$ and $3s$ orbitals. The

contribution of the $3s$ orbital to the $8a_1$ orbital can be assessed by taking the ratio of the atomic

Al Fermi contact term,[41] $b_F(Al) = 3911$ MHz,[42] and the molecular value, $a_F = 958.2(2.3)$ MHz.

This ratio indicates that the $3s$ character of the $8a_1$ orbital is 25%; therefore, the a_1 orbital has

75% $3p_z$ character. This result indicates significant spa_1 hybridization of the valence orbital of

AlC_2. The unpaired electron in the other metal dicarbide radicals studied by rotational

spectroscopy, ScC_2 and YC_2, was also found to be in a hybridized orbital. Because transition

metals are involved, these orbitals were sda_1 hybridized, but with 46-48% s character. The larger

s contribution likely results from greater overlap of the 4s and 5s orbitals of Sc and Y with the C_2

π orbitals, as they are more diffuse than the 3s orbital of Al.[43]

The degree of ionic vs. covalent bonding in AlC_2 can be estimated by calculating the

ionic character i_c via the following equation:[44]

$$eQq = [(1 - i_c)(1 - a_s^2) + 2a_s^2](1 + i_c\varepsilon)2eQq(\text{atom}). \tag{2}$$

Here ε is the screening constant for the p orbital, $eQq(\text{atom})$ is the quadrupole coupling of an

electron in a p orbital for the aluminum atom, and a_s^2 is the percent s character of the bond. For

aluminum, $\varepsilon = 0.35$ and $2eQq(\text{Al}) = -37.52$ MHz,[44] while $a_s^2 = 0.25$ as indicated by b_F.

Assuming $eQq \sim \chi_{aa}$, the ionic character i_c is calculated to be 74%. This high percentage clearly

indicates that the Al-C bond is principally ionic.

It should be noted that with our work, all the rotational spectra of the 3p dicarbide species

(Al – Cl) have been experimentally measured. Therefore, structural trends across the periodic

table can be examined. AlC_2 and SiC_2 are T-shaped, CCP and CCS are linear, and CCCl is

thought to be slightly bent.[10,11,13,45] This change in geometry likely reflects a variation in

bonding, from primarily ionic (Al and Si) to covalent (P and S), and then back again to slightly

ionic (Cl).

Aluminum has a cosmic abundance of Al/H $= 3$ x 10^{-6} – only an order of magnitude

lower than silicon (Si/H $= 4$ x 10^{-5}), but a factor of 10 higher than that of phosphorus (P/H $= 3$ x

10^{-7}).[46] Both CCP and SiC_2 have been detected in the circumstellar envelope of the carbon-rich

star IRC+10216,[3,5] suggesting that AlC_2 is another likely molecule to exist in this object. This study now provides the necessary "rest frequencies" for an astronomical search. The interstellar identification of this radical would be aided by its large dipole moment, calculated to be 4.1 D.[23]

AlC_2 could be synthesized in IRC+10216 by pathways involving acetylene or CCH. The species could be generated via the neutral-atom reaction:

$$C_2H_2 + Al \rightarrow AlC_2 + H_2 \tag{x}$$

This reaction has a rate of 2.5 x 10^{-10} cm^3 s^{-1} at ~50 K.[47,48] Another possible route would be through the CCH radical:

$$CCH + Al \rightarrow AlC_2 + H. \tag{y}$$

No rate information is available for this reaction, but processes involving two radical species can in principle proceed at rates near 10^{-10} cm^3 s^{-1}.[47]

Conclusion

The pure rotational spectrum of aluminum dicarbide, AlC_2, has been measured for the first time, using FTMmmW methods. Highly accurate rest frequencies are now thus available for radio astronomical studies. The data strongly support the T-shaped structure, in agreement with previous theoretical and experimental investigations. The geometry and hyperfine analysis suggest that this species in highly ionic and can be represented as $Al^+C_2^-$. The valance electron appears to be present in an orbital that is spa_1 hybridized, with large $3p_z$ character, also consistent with a T-shaped structure. The degree of ionic vs. covalent character in $3p$ dicarbide species varies considerably from aluminum to chlorine, producing T-shaped, linear, and bent structures. The dicarbide species thus have varied and sometimes unexpected bonding properties.

References

1. J. K. Anderson, and L. M. Ziurys, *Astrophys. J.*, 2014, **795**, L1

2. M. Ohishi, H. Suzuki, S.-I. Ishikawa, C. Yamada, H. Kanamori, W. M. Irvine, R. D. Brown, P. D. Godfrey, and N. Kaifu, *Astrophys. J.*, 1991, **380**, L39

3. D. T. Halfen, D. J. Clouthier, and L. M. Ziurys, *Astrophys. J.*, 2008, **677**, L101

4. S. Saito, K. Kawaguchi, S. Yamamoto, M. Ohishi, H. Suzuki, and N. Kaifu, *Astrophys. J.*, 1987, **317**, L115

5. P. Thaddeus, S. E. Cummins, and R. A. Linke, *Astrophys. J.*, 1984, **283**, L45

6. J. K. Anderson, D. T. Halfen, and L. M. Ziurys, *J. Mol. Spectrosc.*, 2015, **307**, 1

7. C. Yamada, S. Saito, H. Kanamori, and E. Hirota, *Astrophys. J.*, 1985, **290**, L65

8. D. T. Halfen, J. Min, D. J. Clouthier, and L. M. Ziurys, *J. Chem. Phys.*, 2009, **130**, 014305

9. R. Tarroni, *Chem. Phys. Lett.*, 2003, **380**, 624

10. Y. Sumiyoshi, T. Ueno, and Y. Endo, *J. Chem. Phys.*, 2003, **119**, 1426

11. J. Cernicharo, M. Guélin, C. Kahane, M. Bogey, C. Demuynck, and J. L. Destombes, *Astron. Astrophys.*, 1991, **246**, 213

12. J. Min, D. T. Halfen, and L. M. Ziurys, *Chem. Phys. Lett.*, 2014, **609**, 70

13. D. T. Halfen, J. Min, and L. M. Ziurys, *Chem. Phys. Lett.*, 2013, **555**, 31

14. O. Zingsheim, M.-A. Martin-Drumel, S. Thorwirth, S. Schlemmer, C. A. Gottlieb, J. Gauss, and M. C. McCarthy, *J. Phys. Chem. Lett.*, 2017, **8**, 3776

15. V. M. Rayón, P. Redondo, C. Barrientos, and A. Largo, *Chem. Eur. J.*, 2006, **12**, 6963

16. L. Sari, K. A. Peterson, Y. Yamaguchi, and H. F. Schaefer III, *J. Chem. Phys.*, 2002, **117**, 10008

17. B. C. Guo, S. Wei, J. Purnell, S. Buzza, A. W. Castleman Jr., *Science*, 1992, **256**, 515

[18]   S. Wei, B. C. Guo, J. Purnell, S. Buzza, A. W. Castleman Jr., *J. Phys. Chem.*, 1992, **96**, 4166

[19]   A. I. Boldyrev, J. Simons, X. Li, and L. S. Wang, *J. Am. Chem. Soc.*, 1999, **121**, 1019

[20]   L. B. Knight, Jr., S. T. Cobranchi, J. O. Herlong, and C. A. Arrington, *J. Chem. Phys.*, 1990, **92**, 5856

[21]   C. Apetrei, A. E. W. Knight, E. Chasovskikh, E. B. Jochnowitz, and J. P. Maier, *J. Chem. Phys.* 2009, **131**, 064305

[22]   E. Chasovskikh, E. B. Jochnowitz, E. Kim, J. P. Maier, and I. Navizet, *J. Phys. Chem. A*, 2007, **111**, 11986

[23]   J. Yang, R. H. Judge, and D. J. Clouthier, *J. Chem. Phys.*, 2011, **135**, 124302

[24]   X. Zheng, Z. Wang, and A. Tang, *J. Phys. Chem. A*, 1999, **103**, 9275

[25]   M. Sun, A. J. Apponi, & L. M. Ziurys, *J. Chem. Phys.*, 2009, **130**, 034309

[26]   M. Sun, D. T. Halfen, J. Min, B. Harris, D. J. Clouthier, and L. M. Ziurys, *J. Chem. Phys.*, 2010, **133**, 174301

[27]   L. Bizzocchi, B. M. Giuliano, M. Hess, and J.-U. Grabow, *J. Chem. Phys.*, 2007, **127**, 114305

[28]   P. Raghavan, *At. Data. Nucl. Data Tables*, 1989, **42**, 189

[29]   D. Clouthier, private communication

[30]   J. K. G. Watson, *J. Chem. Phys.*, 1967, **46**, 1935

[31]   H. M. Pickett, *J. Mol. Spectrosc.*, 1991, **148**, 371

[32]   J. M. Brown, and T. J. Sears, *J. Mol. Spectrosc.*, 1979, **75**, 111

[33]   W. C. Bowman, and F. C. De Lucia, *J. Chem. Phys.*, 1982, **77**, 92

[34]   A. Largo, P. Redondo, and C. Barrientos, *J. Am. Chem. Soc.*, 2004, **126**, 14611

[35]   Z. Kisiel, *J. Mol. Spectrosc.*, 2003, **218**, 58

36 M. Sun, D. T. Halfen, J. Min, D. J. Clouthier, and L. M. Ziurys, *Chem. Phys. Lett*., 2012, **553**, 11

37 J. S. Robinson, and L. M. Ziurys, *Astrophys. J*., 1996, **472**, L131

38 E. Kostyk, and H. I. Welsh, *Can. J. Phys*., 1980, **58**, 912

39 E. Hirota, Y. Endo, S. Saito, K. Yoshida, I. Yamaguchi, and K. Machida, *J. Mol. Spectrosc*., 1981, **176**, 139

40 S. Rosen, *Spectroscopic Data Relative to Diatomic Molecules*, Pergamon, New York, 1970

41 W. Weltner, Jr., *Magnetic Atoms and Molecules* (Dover, New York, 1983)

42 J. R. Morton, and K. F. Preston, *J. Mag. Reson*, 1978, **30**, 577

43 J. T. Waber, and D. T. Cromer, *J. Chem. Phys*., 1965, **42**, 4116

44 W. Gordy, and R. L. Cook, *Microwave Molecular Spectra*, Wiley, New York, 1984

45 S. Yamamoto, S. Saito, K. Kawaguchi, Y. Chikada, H. Suzuki, N. Kaifu, S.-I. Ishikawa, and M. Ohishi, *Astrophys. J*., 1990, **361**, 318

46 M. Asplund, N. Grevesse, A. J. Sauval, and P. Scott, *Ann. Rev. Astron. Astrophys*., 2009, **47**, 481A

47 D. McElroy, C. Walsh, A. J. Markwick, et al., *Astron. Astrophys*., 2012, **550**, A36: http://udfa.ajmarkwick.net/index.php

48 A. Canosa, S. D. Le Picard, S. Gougeon, et al., *J. Chem. Phys*., 2001, **115**, 6495

Table 1: Measured Transition Frequencies of AlC_2 ($\tilde{X}^2A_1$) in MHz.

$N_{K_a,K_c}{}'$	$\rightarrow$	$N_{K_a,K_c}{}''$	J'	$\rightarrow$	J''	F'	$\rightarrow$	F''	ν_{obs}	$\nu_{obs}-\nu_{calc}$
1_{01}	$\rightarrow$	0_{00}	0.5	$\rightarrow$	0.5	2	$\rightarrow$	3	21732.236	-0.004
			0.5	$\rightarrow$	0.5	3	$\rightarrow$	2	21817.926	-0.002
			1.5	$\rightarrow$	0.5	2	$\rightarrow$	2	21819.145	0.003
			1.5	$\rightarrow$	0.5	4	$\rightarrow$	3	21874.782	-0.003
			1.5	$\rightarrow$	0.5	3	$\rightarrow$	3	21886.038	0.001
			1.5	$\rightarrow$	0.5	1	$\rightarrow$	2	21929.542	0.004
2_{02}	$\rightarrow$	1_{01}	1.5	$\rightarrow$	1.5	2	$\rightarrow$	3	43433.598	0.004
			1.5	$\rightarrow$	0.5	1	$\rightarrow$	2	43497.450	0.000
			1.5	$\rightarrow$	1.5	3	$\rightarrow$	3	43532.306	-0.002
			2.5	$\rightarrow$	1.5	2	$\rightarrow$	1	43535.056	-0.003
			1.5	$\rightarrow$	1.5	3	$\rightarrow$	4	43543.558	-0.002
			1.5	$\rightarrow$	0.5	4	$\rightarrow$	3	43556.837	0.008
			2.5	$\rightarrow$	1.5	3	$\rightarrow$	2	43577.451	-0.001
			2.5	$\rightarrow$	0.5	3	$\rightarrow$	3	43578.667	0.001
			1.5	$\rightarrow$	0.5	2	$\rightarrow$	2	43587.389	-0.002
			2.5	$\rightarrow$	1.5	4	$\rightarrow$	3	43608.016	-0.001
			2.5	$\rightarrow$	1.5	4	$\rightarrow$	4	43619.272	0.002
			2.5	$\rightarrow$	1.5	5	$\rightarrow$	4	43632.991	-0.001
			2.5	$\rightarrow$	1.5	2	$\rightarrow$	2	43645.452	-0.004
3_{03}	$\rightarrow$	2_{02}	3.5	$\rightarrow$	2.5	4	$\rightarrow$	4	65097.008	0.001
			2.5	$\rightarrow$	2.5	4	$\rightarrow$	3	65124.569	-0.003
			3.5	$\rightarrow$	2.5	5	$\rightarrow$	4	65171.148	-0.002
			3.5	$\rightarrow$	2.5	6	$\rightarrow$	5	65191.785	0.004

Table 2: Spectroscopic Constants of AlC$_2$ ($\tilde{X}^2A_1$) in MHz.*

Parameters	This work	Theory [c]	Optical [d]
A	53076.24 [a]	53076.24	52151(14)
B	11950.7408(52) [b]	11946.85	12059.2(9.9)
C	9895.7674(43) [b]	9751.82	9758.2(9.0)
Δ_N	0.90970(95)	0.0140	
Δ_{NK}	0.283 [a]	0.283	
Δ_K	1.42 [a]	1.42	
δ_N	0.00264 [a]	0.00264	
δ_K	0.170 [a]	0.170	
Φ_N	0.000647(51)		
ε_{aa}	65.5 [a]	65.5	
ε_{bb}	80.378(13) [b]	93.95	
ε_{cc}	126.697(20) [b]	148.10	
Δ^s_N	0.0198(15)		
a_F	958.2(2.3)	876.78	947(54)
a_{FD}	-0.0019(12)		
T_{aa}	86.3865(91)	87.8	
$T_{bb} - T_{cc}$	-3.81(60)	-4.08	
χ_{aa}	-32.74(60)	-34.9	
C_{aa}	0.0018	0.0018	
C_{bb}	0.0104(17)	0.0103	
C_{cc}	0.0100(17)	0.0099	
rms	0.003		

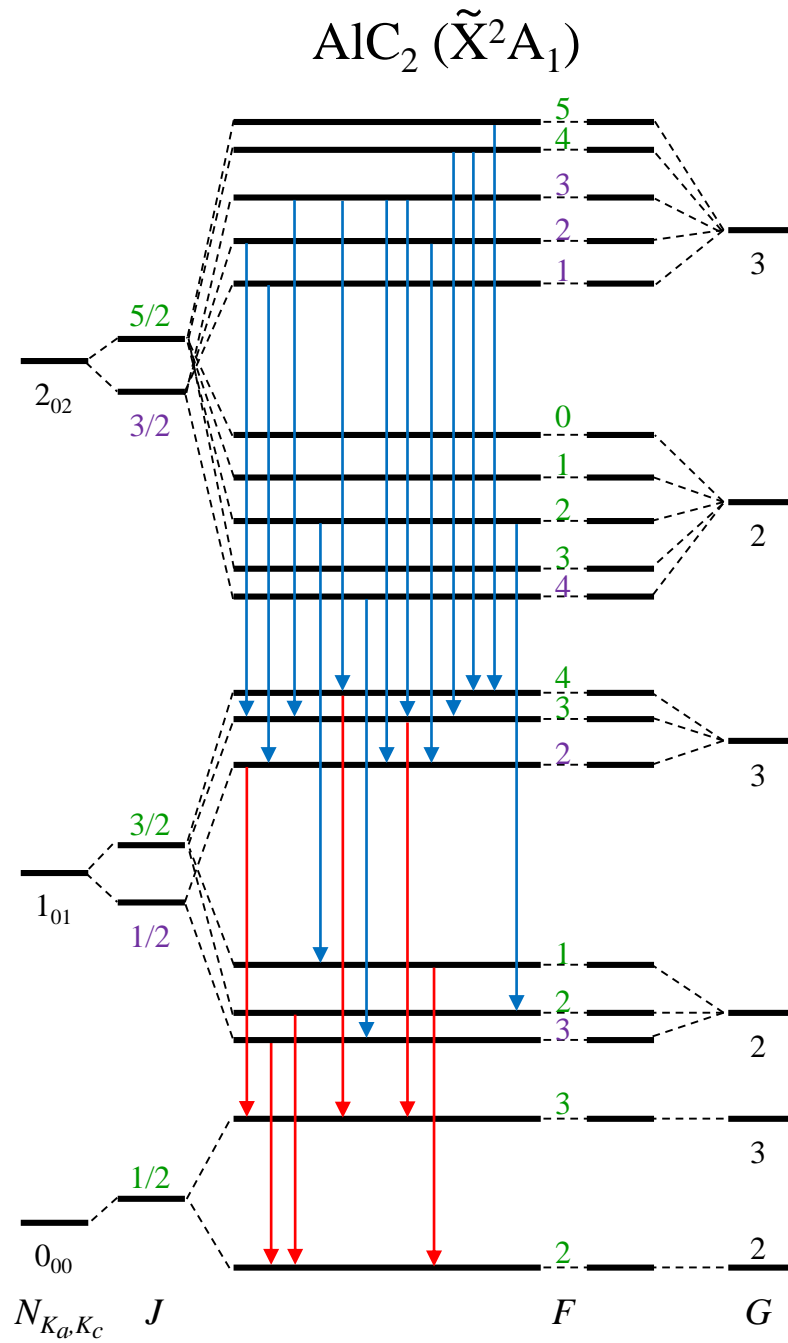* Errors are 3σ in the last quoted decimal places.
[a] Held fixed to theoretical value.　[b] Ratio held fixed to ratio of theoretical values, see text.
[c] B3LYP/aug-cc-pV(5 + d)Z method.[23,29]　[d] Ref. 23.

Figure Captions

Fig. 1 – Energy level diagram of the $N = 0$, 1, and 2 levels of AlC_2 ($\tilde{X}^2A_1$), illustrating the complex fine and hyperfine structure. Levels and quantum numbers in the case b_{β_J} coupling scheme are shown on the left side of the diagram. Here quantum number J indicates the fine structure, where $J = N \pm 1/2$, and F the hyperfine structure arising from the ^{27}Al spin of $I = 5/2$, where $\boldsymbol{F} = \boldsymbol{J} + \boldsymbol{I}$. The right side shows the case b_{β_S} coupling, labeled by quantum numbers G and F, where $\boldsymbol{G} = \boldsymbol{S} + \boldsymbol{I}$ and $\boldsymbol{F} = \boldsymbol{G} + \boldsymbol{N}$. The $N_{K_aK_c} = 1_{01} \rightarrow 0_{00}$ and $2_{02} \rightarrow 1_{01}$ transitions measured in this study are also indicated on the diagram with arrows.

Fig. 2 – Representative FTMmmW spectra of AlC_2 ($\tilde{X}^2A_1$) originating in the $N_{K_aK_c} = 1_{01} \rightarrow 0_{00}$, $2_{02} \rightarrow 1_{01}$, and $3_{03} \rightarrow 2_{02}$ rotational transitions measured near 21 GHz, 43 GHz, and 65 GHz, respectively. The extensive fine/hyperfine structure of this molecule is apparent in these data, labeled by the fine structure quantum number J and the Al hyperfine quantum number F. There are three frequency breaks in each panel to show multiple spectral features. Doppler doublets are indicated by brackets above each line profile. The top panel shows the $N_{K_aK_c} = 1_{01} \rightarrow 0_{00}$ transition, displaying four of the six fine/hyperfine components measured in this work. The middle panel shows four of the 13 lines recorded for the $N_{K_aK_c} = 2_{02} \rightarrow 1_{01}$ transition. The bottom panel presents spectra obtained for the $N_{K_aK_c} = 3_{03} \rightarrow 2_{02}$ transition. The spectra were created from 600 kHz-wide scans, cropped to 500 kHz, each a composite of 1000 – 10,000 pulse averages.

18

$AlC_2\ (\tilde{X}^2A_1)$

AlC$_2$ ($\tilde{X}^2A_1$)

$N_{K_a,K_c} = 1_{01} \rightarrow 0_{00}$

$J = 0.5 \rightarrow 0.5$

$F = 3 \rightarrow 2$

$F = 2 \rightarrow 3$

$J = 1.5 \rightarrow 0.5$

$F = 3 - 3$

$F = 2 \rightarrow 2$

21732.08 21732.33   21817.77 21818.02   21819.00 21819.25   21885.92 21886.17

$N_{K_a,K_c} = 2_{02} \rightarrow 1_{01}$

$J = 1.5 \rightarrow 1.5$
$F = 3 \rightarrow 3$

$J = 2.5 \rightarrow 1.5$
$F = 2 \rightarrow 1$

$J = 1.5 \rightarrow 0.5$
$F = 4 \rightarrow 3$

$J = 2.5 \rightarrow 1.5$
$F = 5 - 4$

43532.17 43532.42   43534.92 43535.17   43556.72 43556.97   43632.88 43633.13

$N_{K_a,K_c} = 3_{03} \rightarrow 2_{02}$

$J = 3.5 \rightarrow 2.5$
$F = 4 \rightarrow 4$

$J = 2.5 \rightarrow 2.5$
$F = 4 \rightarrow 3$

$J = 3.5 \rightarrow 2.5$
$F = 5 \rightarrow 4$

$F = 6 - 5$

65096.85 65097.10   65124.42 65124.67   65171.02 65171.27   65191.65 65191.90

Frequency (MHz)